Mon. Not. R. Astron. Soc. **415,** 2652–2664 (2011) doi:10.1111/j.1365-2966.2011.18891.x

Disc heating: comparing the Milky Way with cosmological simulations

E. L. House,[1⋆] C. B. Brook,[1] B. K. Gibson,[1] P. Sánchez-Blázquez,[1,2] S. Courty,[1,3] C. G. Few,[1] F. Governato,[4] D. Kawata,[5] R. Roškar,[4,6] M. Steinmetz,[7] G. S. Stinson[1] and R. Teyssier[6,8]

[1]*Jeremiah Horrocks Institute, University of Central Lancashire, Preston PR1 2HE*
[2]*Grupo de Astrofísica, Departamento de Fisica Teorica, Universidad Autónoma de Madrid, Cantoblanco E-28049, Spain*
[3]*Centre de Recherche Astrophysique de Lyon, UMR 5574, 9 Avenue Charles André, F69561 Saint Genis Laval, France*
[4]*Astronomy Department, University of Washington, PO Box 351580, Seattle, WA 98195-1580, USA*
[5]*Mullard Space Science Laboratory, University College London, Holmbury St. Mary, Dorking, Surrey RH1 6NT*
[6]*Institute for Theoretical Physics, University of Zürich, CH-8057 Zürich, Switzerland*
[7]*Leibniz-Institue fur Astrophysik Potsdam (AIP), An der Sternwarte 16, 14482 Potsdam, Germany*
[8]*UMR AIM, CEA Saclay, 91191 Gif-sur-Yvette, France*

Accepted 2011 April 8. Received 2011 March 18; in original form 2010 October 12

ABSTRACT

We present an analysis of a suite of simulations run with different particle- and grid-based cosmological hydrodynamical codes and compare them with observational data of the Milky Way. This is the first study to make comparisons of properties of galaxies simulated with particle- and grid-based codes. Our analysis indicates that there is broad agreement between these different modelling techniques. We study the velocity dispersion–age relation for disc stars at $z = 0$ and find that four of the simulations are more consistent with observations by Holmberg, Nordstroem & Andersen in which the stellar disc appears to undergo continual/secular heating. Two other simulations are in better agreement with the Quillen & Garnett observations that suggest 'saturation' in the heating profile for young stars in the disc. None of the simulations has thin discs as old as that of the Milky Way. We also analyse the kinematics of disc stars at the time of their birth for different epochs in the galaxies' evolution and find that in some simulations old stars are born cold within the disc and are subsequently heated, while other simulations possess old stellar populations which are born relatively hot. The models which are in better agreement with observations of the Milky Way's stellar disc undergo significantly lower minor-merger/assembly activity after the last major merger, that is, once the disc has formed. All of the simulations are significantly 'hotter' than the Milky Way disc; on top of the effects of mergers, we find a 'floor' in the dispersion that is related to the underlying treatment of the heating and cooling of the interstellar medium, and the low density threshold which such codes use for star formation. This finding has important implications for all studies of disc heating that use hydrodynamical codes.

Key words: Galaxy: disc – galaxies: evolution – galaxies: formation.

1 INTRODUCTION

One of the major outstanding 'grand challenges' facing astrophysics for the coming decade is the unravelling of the underlying physics governing the formation and evolution of disc galaxies such as our own Milky Way. A principal difficulty resides in trying to accommodate the early collapse and violent merging history intrinsic to the canonical framework of the 'hierarchical assembly' of galactic structure with the apparent stability of what should be fairly fragile thin galactic discs.

High performance computing (HPC) simulations of gravitational *N*-body and hydrodynamical physics have become a primary tool with which to model galaxy formation in a cosmological context (e.g. Katz, Hernquist & Weinberg 1992; Summers, Evrard & Davis 1993; Navarro & White 1994; Steinmetz & Mueller 1994; Abadi et al. 2003a; Sommer-Larsen, Götz & Portinari 2003; Robertson et al. 2004; Bailin et al. 2005; Okamoto et al. 2005; Governato et al. 2007; Gibson et al. 2009; Sánchez-Blázquez et al. 2009; Agertz, Teyssier & Moore 2010). These simulations model the formation and evolution of disc galaxies within a Universe dominated by a

⋆E-mail: elisa.house5@googlemail.com

cold dark matter (CDM) component and a cosmological constant (Λ). While powerful, the techniques employed are not without their problems; for example, the loss of angular momentum in the luminous component of disc galaxies is one of the major problems in most of the aforementioned cosmological simulations. In these simulations, gas cools efficiently via radiative processes, causing baryons to collapse rapidly during the earliest phases of the hierarchical clustering process. The luminous component ends up transferring angular momentum to the dark matter halo, making the luminous component deficient in angular momentum. This is often referred to as the 'angular momentum problem' (Navarro & Benz 1991; Steinmetz & Navarro 2002). As a result, these simulations typically produce galaxies with an overly-dominant spheroid component and an overly-small disc (Abadi et al. 2003a; Scannapieco et al. 2009), in disagreement with observations of disc galaxies (Brook et al. 2004b).

Another challenge facing the disc galaxy formation in the ΛCDM scenario is the old age of the Milky Way's thin disc. This seems at odds with the heating that one expects from merging and accretion events within a ΛCDM paradigm. Indeed, several studies of isolated discs being bombarded by satellites have shown that one would expect that the disc would be destroyed, or at least severely heated, by accretion events (Quinn, Hernquist & Fullagar 1993; Kazantzidis et al. 2008, 2009; Read et al. 2008). Two recent studies have included gas in the main disc, with one (Moster et al. 2010) finding a significant decrease in heating by 25–40 per cent, for gas fractions of 20 per cent and 40 per cent, respectively, with the other (Purcell, Bullock & Kazantzidis 2010) finding that the effects of the gas are somewhat less dramatic. What is clear is that all studies which use contrived initial conditions that are bombarded with satellites are necessarily restricted in their application, both for the discs and for the satellites . For example, how best to assign an appropriate velocity dispersion, mass and scalelength of the Milky Way disc at redshift of 2, say? Were the stars already kinematically 'hot' in this early disc or have they been heated subsequently? Idealized studies with pre-formed discs can be powerful, but they do not address directly the issues pertaining to disc formation and how this relates to merger events as they occur within a hierarchical cosmology. Suffice to say that the existence of thin discs remains a challenge for ΛCDM cosmology. Stewart et al. (2009) argue that gas-rich mergers can explain the number of low-mass galaxies on the blue sequence and mass–morphology relation, but their analysis is not able to address the issue of the thinness of the discs which survive mergers. In fact, it has been shown (Brook et al. 2004b; Springel, Di Matteo & Hernquist 2005; Robertson & Kravtsov 2008; Governato & Brook 2009) that gas-rich mergers in simulations result in hot thick discs, with thin discs forming in the subsequent quiescent period.

Observations of the kinematics of disc stars of our Galaxy have been carried out throughout the years in order to understand the mechanisms governing the formation of the disc. These studies include Nordström et al. (2004) and the follow-up study by Holmberg, Nordström & Andersen (2007), Soubiran & Girard (2005), Soubiran et al. (2008), Quillen & Garnett (2001) and Dehnen & Binney (1998). These studies, however, have provided different pictures of the relationship between the ages of disc stars and their velocity dispersions (the age–velocity dispersion relation). Quillen & Garnett (2001), using the data of Edvardsson et al. (1993), found that vertical disc heating for the Milky Way saturates at $\sigma_w \sim 20$ km s^{-1}, with the value of dispersion virtually constant for stars of ages between $\sim$2 and $\sim$9 Gyr. A discrete jump is apparent for stars with ages $>$9 Gyr which is generally interpreted to be the signature of the thick disc. Thus, this study supports the notion of a thick disc as a separate component to the thin disc and suggests different formation scenarios for each component. By contrast, Nordström et al. (2004) and the follow-up study of Holmberg et al. (2007) advocate a picture in which the disc has undergone continual heating over the past $\sim$10 Gyr. It is not clear from these later studies whether a thick disc should be considered as a separate component: first, the selection is biased towards thin disc stars and, secondly, if the thick disc is a separate component, then it is possible that their result is driven by the increasing contamination of their sample by thick disc stars as older stars are examined (Navarro et al. 2011). One of the main points of contention in such studies, and a possible explanation for the different findings, is the difficulty in determining the ages of stars (Anguiano et al. 2009; Aumer & Binney 2009). Further, Seabroke & Gilmore (2007) showed that a power-law fit as suggested in the Geneva-Copenhagen studies is statistically similar to disc-heating models which saturate after $\sim$4.5 Gyr and is consistent with a minimal increase of σ_w for old stars. We will compare our simulations to both these data sets.

The degree of the heating of thin disc stars is certainly complicated by an old, hot 'thick disc' of stars. Since the discovery of the thick-disc component of the Milky Way by Gilmore & Reid (1983), several analyses of ages, abundances and kinematics have indicated that the thick and thin discs are two distinct components (e.g. Reid & Majewski 1993; Nissen 1995; Chiba & Beers 2000; Bensby et al. 2007; although see Ivezić et al. 2008 for an opposing view), where a thin disc whose stars have formed continuously over $\sim$9 Gyr is superimposed on an old thick disc. The thick disc has also been shown to be a common component in most, and possibly all, observed spiral galaxies (Yoachim & Dalcanton 2008), at least in the sense that the light distributions are better fitted by two functions rather than one. Recent observations carried out by measuring the stellar population of the Milky Way's thick disc give scaleheights that range between 500 and 1100 pc (Jurić et al. 2008; Carollo et al. 2010) compared to the thin disc that has a measured scaleheight in the range 200–400 pc (Jurić et al. 2008; Carollo et al. 2010). The rotational lag of the thick disc of the Milky Way ranges from 20 km s^{-1} (Chiba & Beers 2000) to 50 km s^{-1} (Soubiran et al. 2008). The velocity ellipsoid (i.e. the velocity dispersions in the u,v,w reference frame) of the thick disc has been quoted as being from (σ_u, σ_v, σ_w) = (46 $\pm$ 4, 50 $\pm$ 4, 35 $\pm$ 3) km s^{-1}, as measured by Chiba & Beers (2000), to (σ_u, σ_v, σ_w) = (63 $\pm$ 6, 39 $\pm$ 4, 39 $\pm$ 4) km s^{-1}, as measured by Soubiran et al. (2008). The thin disc dominates the thick disc in the local region by a factor of 10:1 in terms of stellar mass, but the difficulty in determining scalelengths of the two means that comparing their total masses is highly uncertain, with estimates ranging from the mass ratio 10:1 to 3:1 (Jurić et al. 2008).

For this study, we focus on the kinematics and heating of all stars within the disc region of our simulations, without any a priori distinction between the thin and thick discs. We will explore and discuss occasions where two components arise, in the hope of shedding light on the various scenarios which have been postulated to explain the formation of the thick and thin discs. One model suggests that a previously existing thin disc was kinematically heated to give rise to a thick disc. This vertical heating of the thin disc stars could be rapid, due to mergers (Quinn et al. 1993), or more gradual, as a result of secular processes such as giant molecular clouds, spiral arms or the presence of a bar providing the necessary kinematic 'kick' to the stars (Larson 1976). An alternative model suggests that the thick disc formed during the violent relaxation of the galactic potential prior to the formation of the thin disc,

where star formation was triggered by the accretion of gas during major merger events at an early epoch (Brook et al. 2004b). This raises the question of whether the age–velocity dispersion relation is at least in part due to the earlier discs being, in general, hotter than the later discs, that is, the old stars were born hotter than the younger stars, possibly related to earlier mergers in ΛCDM having higher mass ratios between the mass of the central galaxy and that of the accreted satellite in general than later mergers (Brook et al. 2005). Recent observations suggesting that high-redshift discs are relatively thick (Dalcanton & Bernstein 2002; van Starkenburg et al. 2008; Lemoine-Busserolle & Lamareille 2010) possibly provide support for this scenario. A further alternative model suggests that the thick disc stars are actually accreted from satellite galaxies during the hierarchical assembly process (Abadi et al. 2003a). Recently, models of discs which are entirely isolated from the satellite bombardment that is predicted in ΛCDM have shown that the migration of stars can naturally lead to combinations of age, metallicity and dispersions which are consistent with observations of thin- and thick-disc populations (Loebman et al. 2010 as well as an analytic model by Schönrich & Binney 2009). These models beg the question of whether heating is required at all; yet to be fair, they have not been integrated within a fully cosmological paradigm. Finally, Kroupa (2002) suggested that massive star clusters formed at high redshift dissolve at later times to form the thick disc, a theory given support by the clumpy nature of high-redshift discs (Elmegreen & Elmegreen 2006; Elmegreen 2007).

We aim to provide further insight into the causes of the age–velocity dispersion relation of all disc stars (thick and thin) by using a suite of HPC simulations of disc galaxies, each run with a different hydrodynamical code, different initial conditions, different resolution and different assembly histories, to sample a wide range of disc galaxy formation pathways. In particular, we determine whether disc stars are born hot or cold in early times, and the degree to which they subsequently heat vertically. Attention is given to any connection between heating rates and accretion histories. The issue of the effects of numerical heating is important in all studies of disc heating. We show that numerical heating is not causing the measured disc heating. We highlight the role of the implementation of star formation recipes, and the modelling of the interstellar medium (ISM) in which stars are formed, as determinants of a dispersion 'floor' for the simulations.

In Section 2, we briefly describe the main characteristics of each of the different codes used to produce our compilation of simulations. In Section 3, we present our main results which include the dispersion of all stars as a function of time for the final galaxies, comparing the simulations with observations of the Milky Way, studying the kinematics of young stars at different epochs, as well as following the heating of stars born at early epochs; we then relate the heating with merger processes within the simulations. In Section 4, we examine isolated simulations and show that heating does not occur in the absence of a cosmological environment, ruling out numerical effects as the primary agent driving our results. We present our conclusions in Section 5.

2 THE SIMULATIONS

We analyse seven cosmological disc simulations run with different *N*-body hydrodynamical galaxy formation codes. In this section, we provide a summary of the main details of each code. For full details, references are provided.

Two of the simulations we analysed in this study are run with RAMSES (Teyssier 2002), which models the gas hydrodynamics using an adaptive mesh refinement (AMR) scheme, while the other codes use a smoothed particle hydrodynamics (SPH) approach.[1] Using examples drawn from these different fundamental approaches should provide greater confidence in the robustness of our results. To the best of our knowledge, our study is the first to compare properties of simulated disc galaxies formed using these two commonly adopted methodologies.

All five simulations[2] have cosmological initial conditions where small-scale structures merge to form increasingly larger objects in the Universe as part of the so-called hierarchical framework. They all have a similar Milky Way type mass halo and all the different codes self-consistently include the primary physical processes needed to model galaxy formation and evolution. These consist of the effects of gravity, hydrodynamic pressure and shocks, star formation and feedback, radiative cooling, and a photoionizing ultraviolet background. They all adopt a type of Schmidt law for converting gas particles into stars, where the star formation rate (SFR) is proportional to the gas density to some power.

The main difference between the simulations is that they have different initial conditions, and hence merger and assembly histories. They also adopt different recipes for feedback from Type II supernovae (SNeII). Various methods have been suggested to incorporate the SN feedback into numerical simulations: one technique is to artificially turn-off radiative cooling in the area where a SNII explosion occurs for a time-scale long enough to allow the blast wave to expand. We call this type of feedback 'adiabatic feedback'. The second approach is to directly inject kinetic energy into the surrounding gas; we refer to this as 'kinetic feedback'. Two of our simulations use kinetic feedback, while the rest use an adiabatic approach. Pure 'thermal feedback' is used in the case of SNeIa, where the longer lifetimes of the progenitors (relative to SNeII) mean that the energy is not released into the same high-density regions from which the stellar particles formed (and hence, the associated energy is not radiated away as efficiently as for the case of SNeII).

Each of the simulations employs star formation recipes which are similar; stars can form only from gas above a certain density threshold. Since cosmological simulations typically lack resolution below a few hundred parsecs, this sets a maximum density that the simulations can resolve of the order of $0.1\,\mathrm{cm}^{-3}$; all of the simulations here adopted this star formation threshold. We shall discuss the impact of this threshold selection later in this paper.

The main properties of each of our simulations are presented below and summarized in Table 1.

2.1 S09_YCosm_AMR_RAMSES

We ran a high-resolution fully-cosmological (YCosm) disc simulation to redshift zero using the AMR-based code RAMSES (Teyssier 2002). The SN feedback is modelled by directly injecting kinetic energy into the surrounding gas, that is, kinetic feedback.

This simulation (hereinafter referred to as S09) was run within a 'concordance' cosmology framework, with $\Omega_0 = 0.3$, $h_0 = 0.7$, $\Omega_\mathrm{b} = 0.045$ and $\Omega_\Lambda = 0.7$. A preliminary analysis for this simulation was presented in Gibson et al. (2009), while its optical

[1] Knebe (2005) provides an excellent primer to the differences between the particle- and grid-based approaches to solving Poisson's equation, in an *N*-body context.

[2] As we mention below, we actually analyse six simulations, but one of these is simply a higher resolution version of one of the base simulations, and so is not entirely 'independent'. We also include in our analysis a non-cosmological simulation (see Section 2.7).

Table 1. Summary of the properties for the simulation suite.

Simulation name	Code	$M_{\rm vir}$ ($M_\odot$)	Ω_0	h_0	$\Omega_{\rm b}$	$t_{\rm LMM}$ (Gyr)	ϵ (kpc)	Gas resolution ($M_\odot$)	Feedback
S09	RAMSES	7.6×10^{11}	0.3	0.7	0.045	10.99	0.4	1.0×10^6	Kinetic
G07 (MW1)	GASOLINE	1.1×10^{12}	0.3	0.7	0.039	10.89	0.6	8.0×10^5	Adiabatic
B09 (h277)	GASOLINE	7.1×10^{11}	0.24	0.77	0.045	10.41	0.35	1.6×10^4	Adiabatic
B05 (SGAL1)	GCD+	5.0×10^{11}	1	0.5	0.1	9.74	0.6	1.0×10^6	Adiabatic
A03	GRAPESPH	9.4×10^{11}	0.3	0.65	0.045	8.31	0.5	2.0×10^6	Kinetic
H09	RAMSES	7.6×10^{11}	0.3	0.7	0.045	10.99	0.2	1.3×10^5	Adiabatic
R08	GASOLINE	1.0×10^{12}	0.3	0.7	0.039	N/A	0.05	0.2×10^5	Adiabatic

properties were categorized extensively by Sánchez-Blázquez et al. (2009). The simulated disc had its last major merger (LMM, defined as having the total mass ratio of 1:3 or higher) at a redshift of $z = 2.6$, that is, $t_{\rm LB} = 10.99$ Gyr (where $t_{\rm LB}$ = look-back time); however, interactions with smaller satellites still occur at lower redshifts. We discuss the LMM later in this paper. Its final virial mass is 7.6×10^{11} $M_\odot$ at $z = 0$.

2.2 G07_MW1_YCosm_SPH_GASOLINE

This simulation is denoted by MW1 in the work of Governato et al. (2007) [hereinafter referred to as G07(MW1)]. The code used for this fully-cosmological (YCosm) simulation is the SPH code GASOLINE (Wadsley, Stadel & Quinn 2004). The SN feedback mechanism uses an adiabatic feedback approach where cooling was stopped artificially to allow blast waves from SNe to expand and heat the surrounding ISM. In all the simulations run with GASOLINE presented here, 40 per cent of the SN energy is coupled to the surrounding gas. Such a prescription results in a decrease in the amount of the gas cooling early in the galaxy's formation, reducing the loss of angular momentum resulting from the merging of dense stellar systems.

The simulation employed was run within a concordance cosmology with $\Omega_0 = 0.3$, $h_0 = 0.7$, $\Omega_{\rm b} = 0.039$ and $\Omega_\Lambda = 0.7$; the LMM was at redshift $z = 2.5$, that is, $t_{\rm LB} = 10.89$ Gyr, with several late minor interactions thereafter. The final virial mass is 1.1×10^{12} $M_\odot$.

2.3 B09_h277_YCosm_SPH_GASOLINE

This simulation was also run with GASOLINE and was previously studied in Brooks et al. (2009) [hereinafter referred to as B09(h277)]. The simulation was run in a concordance cosmology, with $\Omega_0 = 0.24$, $h_0 = 0.77$, $\Omega_{\rm b} = 0.045$ and $\Omega_\Lambda = 0.76$. The redshift of its LMM is also at $z = 2.5$, that is, $t_{\rm LB} = 10.41$ Gyr, but unlike the case for G07(MW1), this simulation experiences no mergers or accretion events since $z \approx 0.7$ or $t_{\rm LB} = 5.8$ Gyr. The force resolution is also somewhat higher than that for G07(MW1).

2.4 B05_SGAL1_NCosm_SPH_GCD+

This simulation was taken from the work of Brook et al. (2005) [hereinafter referred to as B05(SGAL1)]. The SPH code GCD+ (Kawata & Gibson 2003) was employed, although this particular run was not fully cosmological (NCosm). Semi-cosmological models, like B05(SGAL1), consist of an isolated sphere of dark matter and gas instead of a large cosmological volume. Small-scale fluctuations are superimposed on the sphere to allow for local collapse and subsequent star formation. Solid body rotation is also applied to the sphere to incorporate the effects of longer wavelength fluctuations that a semi-cosmological model does not otherwise account for. Feedback from SNeII was assumed to be adiabatic, with cooling turned off in the surrounding gas.

The cosmological framework in which B05(SGAL1) was run is quite different from that of the simulations discussed thus far; specifically, it used $\Omega_0 = 1$, $h_0 = 0.5$, $\Omega_{\rm b} = 0.1$ and $\Omega_\Lambda = 0$. While using the currently favoured ΛCDM framework would have a significant impact upon simulations of large-scale structure formation from Gaussian random noise initial conditions, it has been shown that, within the context of single galaxy formation models, such as B05(SGAL1), the resulting differences are negligible (Brook et al. 2005). In terms of its merger history, B05(SGAL1) is not dramatically different from B09(h277), in the sense that their is little or no merger activity since redshift $z \approx 0.5$ or $t_{\rm LB} = 5.9$ Gyr.

2.5 A03_YCosm_SPH_GRAPESPH

This simulation (hereinafter referred to as A03) was first presented in Abadi et al. (2003a). It is a fully-cosmological (YCosm) Milky Way like disc galaxy, simulated with the GRAPESPH code (Steinmetz 1996). Feedback is predominantly thermal, with 5 per cent of SN energy converted into kinetic feedback and injected into the surrounding gas particles. A flat ΛCDM cosmology was assumed, with $\Omega_0 = 0.3$, $h_0 = 0.65$, $\Omega_{\rm b} = 0.045$ and $\Omega_\Lambda = 0.7$. Its final virial mass was 9.4×10^{11} $M_\odot$ and its LMM occurred at $z = 1$, that is, $t_{\rm LB} = 8.31$ Gyr, although a number of minor interactions occur thereafter.

2.6 H09_YCosm_AMR_RAMSES

This simulation (hereinafter referred to as H09) traces the same halo as S09 described in Section 2.1, but runs with a higher spatial resolution and employs a different feedback mechanism for SNeII. Instead of using kinetic feedback as in S09, it relies on an adiabatic feedback scheme.

2.7 R08_NCosm_SPH_GASOLINE

This simulation (hereinafter referred to as R08) is taken from Roškar et al. (2008). It is an isolated Milky Way type disc galaxy (1.0×10^{12} $M_\odot$) with solid body rotation added, similar to the B05(SGAL1) simulation; R08 differs from the latter in that R08 does not incorporate small-scale density fluctuations. This means that this isolated simulation experiences no merger or accretion events. It is evolved for 10 Gyr using the same GASOLINE code as G07(MW1) and B09(h277), but at extremely high spatial resolution (softening length of 50 pc).

3 RESULTS

For observed solar neighbourhood stars, it is well established that there is a relationship between their velocity dispersion and age. We refer to the increase in the dispersion with time as *disc heating*, where the relationship for the solar neighbourhood indicates that the older disc stars are kinematically 'hotter' than their younger counterparts. Examining the dynamics of stars as a function of time therefore contains valuable information about the heating processes – driven by some combination of secular and satellite merger-driven phenomena. We focus on the vertical heating (σ_w, perpendicular to the plane of the galaxy) as this out-of-plane heating is more susceptible to mergers/interactions. In-plane heating (σ_u and σ_v) is more sensitive to spiral wave and bar-driven heating which we do not consider in our study.[3]

In what follows, we first examine the velocity dispersion–age relation, similar to the manner in which observers study the same relation within the Milky Way, but now for stars within the simulated discs at $z = 0$. However, since the dispersion of stars at $z = 0$ does not provide direct information as to the velocity dispersion of the population *at birth*, we extend our analysis to study the time-evolution of the heating of subpopulations of disc stars. Thereafter, specifically, we will attempt to ascertain whether stars which are kinematically hot *today*were born 'hot' or were born 'cold and heated' (by whatever means).

3.1 Age–velocity dispersion relation

We first examine the velocity dispersion perpendicular to the plane of the galaxy (σ_w) for all stars at $z = 0$ within the 'local' disc, which we define as $7 < R_{xy} < 9$ kpc and $|z| < 1$ kpc, as a function of age (Fig. 1).[4] With such a selection function, all the simulations show little in the way of evidence for stellar heating for young stars with ages ∼1 to ∼3 Gyr, as well as much higher dispersions for old stars (consistent with observations of the Milky Way).

We should point out that for the semi-cosmological simulation, B05(SGAL1), we used a slightly larger radial cut of $4 < R_{xy} < 8$ kpc and $|z| < 1$ kpc due to the smaller number of star particles in this particular run. We found that in the smaller region of $7 < R_{xy} < 9$ kpc, there were not enough stars for some age bins to measure an accurate velocity dispersion. We were therefore forced to use a larger region for this simulation. However, we also tested our results in all the simulations for three different radial cuts to ensure that the trends remain the same independent of the radius.

The S09 and H09 simulations show little sign of heating for stars younger than ∼3 Gyr; for older stars, several discrete 'jumps' in velocity dispersion can be discerned. Similar trends and small discrete jumps are also seen in the G07(MW1) simulation, in addition to a discontinuity in the dispersion for stars of age ∼8 Gyr. The latter can be traced to a period of enhanced merger activity early in the galaxy's evolution, just prior to the establishment of its stable disc.

Like all the simulations, A03 also shows dispersion trends consistent with the signature of continual/secular heating at later times. Stars older than ∼9 Gyr, in particular, possess a significantly large velocity dispersion. These high dispersions are a signature of the so-called 'angular momentum problem' mentioned in Section 1, which results in the formation of an overly-dominant spheroid compared to observations. The spheroid component is dominated by old stars which are ultimately the agents responsible for the production of the high dispersions seen to the right-hand side of Fig. 1.

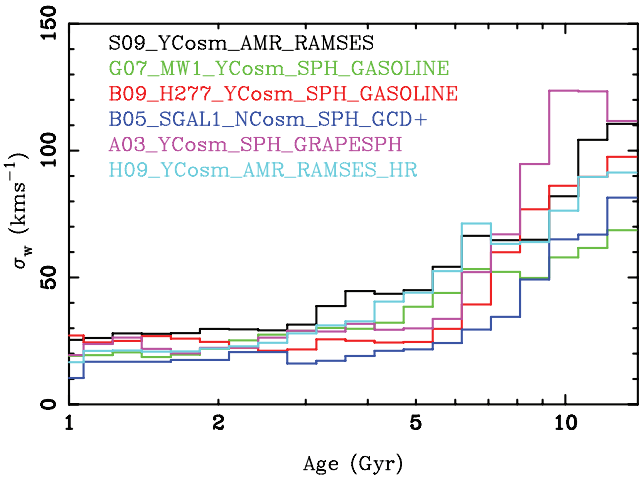

Figure 1. Age–velocity dispersion relation in the vertical direction for 'local' disc stars in our suite of simulations.

The absence of significant heating seen in all simulations for stellar ages of ∼1–3 Gyr extends to somewhat older stars (up to ∼6 Gyr in age), for both the B09(h277) and the B05(SGAL1) simulations. For older stars, discrete jumps in the dispersion, superimposed upon a continual heating profile, are evident. The longer period during which stars show little heating is reminiscent of the Quillen & Garnett (2001) interpretation of extent observations that this reflects 'saturation' in the thin disc's kinematic heating. The older, kinematically hotter, stars in these simulations have been suggested to be a signature of the thick disc (e.g. Brook et al. 2004b).

Broadly speaking, while there is a continuum of heating 'profiles' on display in Fig. 1, at one end of the spectrum, several of the simulations [e.g. S09, H09, G07(MW1)] show a temporal heating profile which becomes apparent at younger ages (∼3 Gyr) relative to several at the opposite end of the spectrum [e.g. B05(SGAL1), B09(h277)] which only begin to show evidence of significant heating in older stars (>6 Gyr). If we associate these relatively flat periods at late times with the thin disc, then none of the simulations has thin discs as old as that of the Milky Way, which is considered to be 8–10 Gyr old.

One of the natural consequences of the merging which occurs within the hierarchical clustering paradigm is a degree of kinematical heating. As such, we set out to examine the merging histories for each of the simulations, to see whether they shed light on the characteristic heating profiles and discrete 'jumps' seen in the age–velocity dispersion plane (Fig. 1); these merging histories will be discussed shortly.

One thing which is readily apparent from our analysis is that *all* of the simulations show much higher velocity dispersions for the older stars in the disc, consistent with the behaviour seen in the Milky Way. That said, there is also a consistent offset, in the sense that all of the simulated discs are substantially hotter than that of the Milky Way. Part of this discrepancy relates to the fundamental problem alluded to in Section 1, specifically, that gas cools efficiently allowing baryons to collapse early during the merging process of galaxy formation, resulting in unrealistically large spheroidal

[3] Further, Seabroke & Gilmore (2007) showed that dynamical streams can contaminate the local in-plane velocity distributions, which can complicate and compromise the comparison with simulated in-plane velocity distribution functions which do not capture adequately structure on that scale.

[4] In the sense that 'young stars' have 'small ages', in Fig. 1, and 'old stars' have 'large ages'.

components. These old spheroidal stars can have a significant impact on the derived dispersions, in the sense of 'contaminating' what one would like to be a 'pure' disc sample. In other words, rather than measuring the dispersion of disc stars, which reflects the observational case, one is instead probing the additional impact that the dispersion of the spheroid stars has upon the sample. This is problematic, at some level, for all of the simulations – it is reflected in the very high dispersions seen at large ages in Fig. 1. In order to make a fair comparison with disc stars from the Milky Way, we clean (in a very straightforward manner) our sample off these spheroidal contaminants by selecting *in situ* stars, that is, those that are born in the central galaxy. These *in situ* stars are identified as those which form anywhere within the central galaxy, while stars that end in the central galaxy at $z = 0$ but were born within a satellite or substructure are called *accreted*. We then derive the velocity dispersions of *in situ* stars in our defined disc region , $7 < R_{xy} < 9$ kpc and $|z| < 1$ kpc, at $z = 0$.

By selecting *in situ* stars we are examining the heating of disc stars. Whether this results in forming the thick disc or merely the old, hot thin disc is left open to interpretation. Of the thick disc formation mechanisms proposed (see Section 1), the direct accretion of satellites scenario is thus not explicitly addressed in this study. In this analysis, we merely assume that a rotationally supported disc forms *in situ* and can be born relatively hot or cold, and then may be heated by a number of processes. Further, recent simulation results have shown that some *in situ* stars will form part of the stellar halo (Zolotov et al. 2010) and thus may affect our dispersion results. However, these stars are in the halo, with too few in our defined disc region to affect the velocity dispersion–age plots presented here.

We plot in Fig. 2 the age–velocity dispersion relation of these *in situ* stars from the simulations along with three sets of observational data for the Milky Way disc: Quillen & Garnett (2001), a combined set from Soubiran & Girard (2005) and Soubiran et al. (2008), and Holmberg et al. (2008). Quillen & Garnett (2001) use a sample of 189 nearby F and G dwarfs from Edvardsson et al. (1993); from their resulting velocity dispersion–age relation, they suggest that the Milky Way disc has been relatively quiescent with little heating for stars with ages between 3 and 9 Gyr, with stars older than that having been subject to an abrupt heating event. The second set of observational points is taken from Soubiran & Girard (2005) and Soubiran et al. (2008). We have merged these two catalogues, in order to include a larger number of old disc stars in the sample. We note that these data include the Reddy et al. (2003), Bensby, Feltzing & Lundström (2003) and Bensby, Feltzing & Lundström (2004) samples, which target the thick disc specifically by using a kinematic selection, and this may be the reason why their old stars are hotter than in the Holmberg et al. (2008) samples. Their analysis is consistent with that of Quillen & Garnett (2001), where the age–velocity dispersion relation of the thin disc is characterized by the saturation of the vertical dispersion at ∼25 km s^{-1} at ages ∼4–5 Gyr. The final set of observations is that from Holmberg et al. (2008); they present a sample of F and G dwarfs from the Geneva–Copenhagen Survey of the solar neighbourhood (Nordström et al. 2004), suggestive of a scenario consistent with the continual heating of the local disc throughout its lifetime.

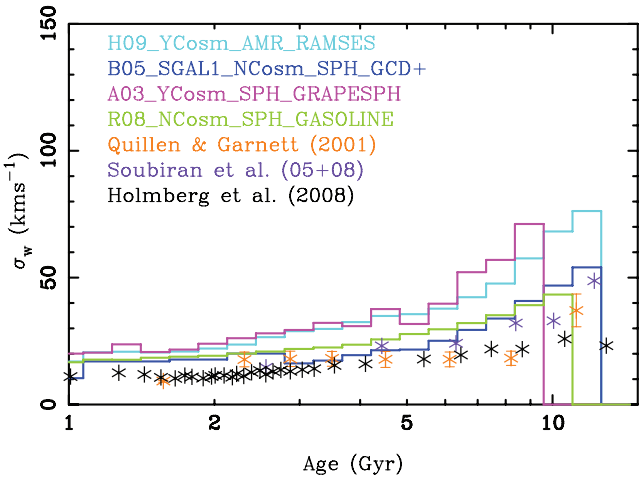

Figure 2. Vertical age–velocity dispersion relation for *in situ* disc stars within our suite of simulations, compared with observations from Quillen & Garnett (2001), Soubiran & Girard (2005), Soubiran et al. (2008) and Holmberg et al. (2008).

By considering only *in situ* disc stars, we have eliminated a significant fraction of the high dispersion old spheroidal components' contaminants; this is reflected in the ∼20–30 per cent decrease in σ_w for stellar ages in excess at ∼7–8 Gyr. We have only included four of the simulations in Fig. 2, although the results that follow apply to the entire suite. The overall trend in Fig. 2 matches that of Fig. 1, in the sense that a range of heating 'profiles' are seen, with both continual and discrete events being evident.

We also compared the velocity dispersions in Fig. 2 in three different regions for our highest resolution simulations [H09, R08 and B09(h277), with the selected regions being $4 < R_{xy} < 8$ kpc, $6 < R_{xy} < 9$ kpc and $7 < R_{xy} < 9$ kpc]. These simulations have enough stars to examine much smaller volume cuts. We found that the trends in velocity dispersion remain the same, independent of the radial cut, with quantitative differences from Fig. 2 being insignificant.

It might be argued that the three simulations with the (relatively) oldest disc component [B09(h277), B05(SGAL1) and R08] – also, those with relatively flat velocity dispersion–age relations for ages up to ∼6 Gyr – are a somewhat better reflection of the relation inferred from the observations. We will show in Section 3.3 that the merger history of these systems is a primary driver in the establishment of this relationship and examine the role played by numerical effects.

An interesting observation from Fig. 2 is that there is a significant offset, even when including just *in situ* stars, with all simulations compared with observations at any time in the galaxy's evolution, in the sense that the stars in the simulations are hotter than the observed stars at all times [with the exception of the semi-cosmological simulation B05(SGAL1)]. This offset is particularly high when looking at old stars but is also significant for young stars. Several possibilities might be responsible for driving such a discrepancy: (i) numerical heating due to limited force resolution; (ii) the treatment of heating and cooling within the ISM of the simulations; and (iii) the adopted low star formation threshold.

The issue of numerical heating will be addressed at length in Section 4; here, we simply note that the offset also exists in the simulation of Roškar et al. (2008), which has a force resolution of 50 pc, and it also exists in other high-resolution isolated disc simulations in the literature (e.g. Kazantzidis et al. 2008, 2009; Stewart et al. 2009). In Fig. 2, one can view our highest resolution simulation (R08), as well as our lowest [B05(SGAL1)]; if numerical heating were the main agent of the observed offset between the simulations and observations, one might expect the lowest resolution simulation to be (kinematically) the hottest. This is not the case though and, in fact, B05(SGAL1) has the lowest resolution and is the coldest in the sample.

Another important aspect to consider is the effect of secular heating; R08 has sufficient resolution to account for heating from internal processes such as from spiral arms. As the simulation is isolated and therefore removed from a cosmological context, the observed heating profile in this simulation must be secular due to spiral arms directly heating stars as well as causing migration (Loebman et al. 2010). For the R08 simulation, these internal heating processes *alone*are enough to match the observations of Holmberg et al. (2008).

3.2 Are stars born hot or heated subsequently?

In this section, we aim to answer several questions that emerged from the above kinematical analysis of $z = 0$ stars: were the kinematically hot, old stars in Figs 1 and 2 born with these high velocity dispersions, or were they born 'cold' and heated subsequently? If the latter, then what is the source of this heating? To answer these, we examine the kinematics of disc stars at the time of their birth for different epochs of galaxy formation. We do this by selecting disc stars born in the 'disc' region, $4 < R_{xy} < 8$ kpc and $z < 1$ kpc, at the time of their birth, using a fairly arbitrary time 'slice' of 200 Myr, that is, we are deriving the velocity dispersion of young disc stars in each simulation at various epochs. We tested our results with different radial cuts and age ranges, and found that our results and conclusions are not sensitive to the used values. The slightly larger radial slice used in this section allows us to obtain a larger sample of stars to derive their dispersions.

Fig. 3 shows the derived velocity dispersions for young stars at different times throughout the respective simulations' evolution. Each of the orthogonal components of σ are highlighted, although as noted earlier, our analysis will concentrate solely upon σ_w. For clarification, stars born at early times are situated to the left-hand side of each panel in Fig. 3, while stars born more recently are located towards the right-hand side, that is, the abscissa now reflects 'cosmic time' rather than 'stellar age' (as was employed in Figs 1 and 2).

For the S09 simulation (top left-hand panel of Fig. 3), all disc stars, independent of time, are born cold with low vertical velocity dispersions of $\sigma_w \approx 30\,\mathrm{km\,s^{-1}}$, on average. There is a slight increase in the dispersion for stars with formation times between ∼7 and 10 Gyr, where the dispersion increases by ∼25 per cent. This epoch corresponds to a period of enhanced minor merger activity, during which the ISM is heated kinematically relative to the adjoining quiescent phases.

For the G07(MW1) simulation (top middle panel of Fig. 3), stars are born on average with vertical velocity dispersions between $\sigma_w = 20$ and 30 $\mathrm{km\,s^{-1}}$, except for the period between ∼3 and 5 Gyr. During this time there are several minor mergers with satellites which result in these stars being born with velocity dispersions roughly twice that of the adjoining phases ($\sigma_w = 60\,\mathrm{km\,s^{-1}}$). It is also important to note that these mergers produce a short-lived warp at $z = 2$, that is, at $t = 3.2$ Gyr. The stars that we detected in the disc during this period were located within this warp region. Because of their potential to dominate over in-plane stars at only a few scalelengths, stars in the warp should be treated carefully, particularly in the case of studying their kinematics, as they can result in an apparent increase in the velocity dispersion (Roškar et al. 2010). These 'warp' stars are kinematically 'disturbed' and born with higher σ_w. This is a very similar trend to that seen in the H09 simulation (bottom right-hand panel of Fig. 3) where stars, on average, tend to have dispersions between $\sigma_w = 20$ and 30 $\mathrm{km\,s^{-1}}$ at the time of birth, but there is a period between ∼3 and 5 Gyr, again, where this dispersion doubles to about $\sigma_w = 60\,\mathrm{km\,s^{-1}}$. As for G07(MW1), this period coincides with an epoch of enhanced satellite interaction with the main galaxy, although in G07(MW1) the warp is the primary cause of the high velocity dispersion during this period and not the minor mergers.

A distinct trend is noted for the B09(h277), B05(SGAL1) and A03 simulations. Stars born at late times (over the past ∼6 Gyr) are born cold, with velocity dispersions between 10 and 20 $\mathrm{km\,s^{-1}}$, while stars born prior to this are born hot (with vertical velocity dispersion of ∼70 $\mathrm{km\,s^{-1}}$). It is tempting to interpret this as the signature of separate thin and thick discs, where the thick disc is composed of older stars which were born hotter than the younger, colder, thin disc (Brook et al. 2004b).

The high velocity dispersion measured at early times in A03, that is, from ∼2 to 6 Gyr, is due to the numerous merger events that

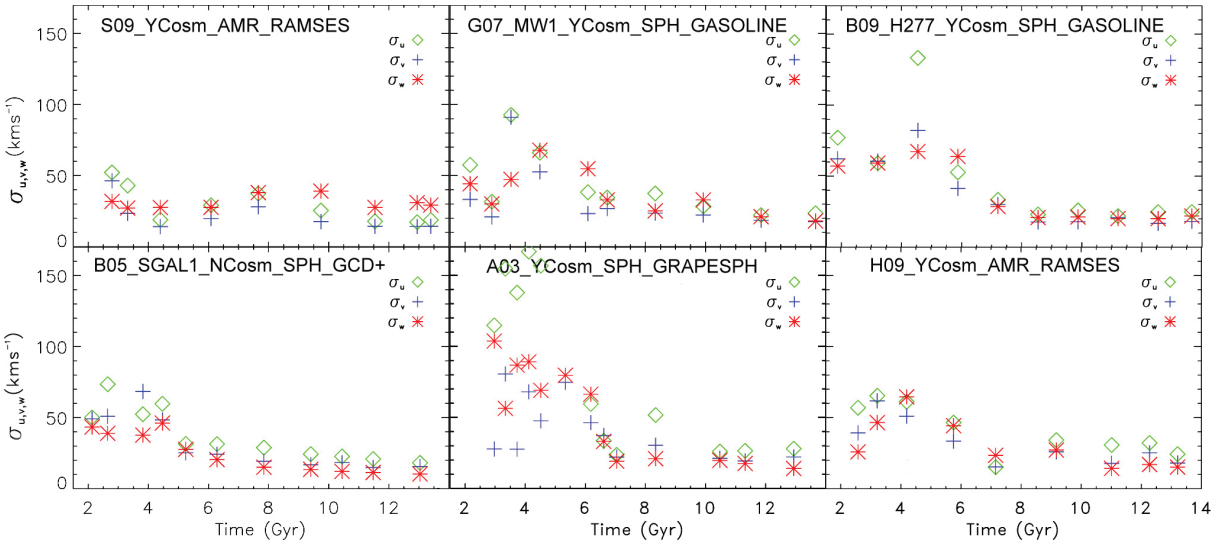

Figure 3. Radial, tangential and vertical velocity dispersion components (σ_u, σ_v and σ_w, respectively) for young stars (<200 Myr) at the time of their birth for different epochs, within the defined disc annulus $4 < R_{xy} < 8$ kpc and $|z| < 1$ kpc.

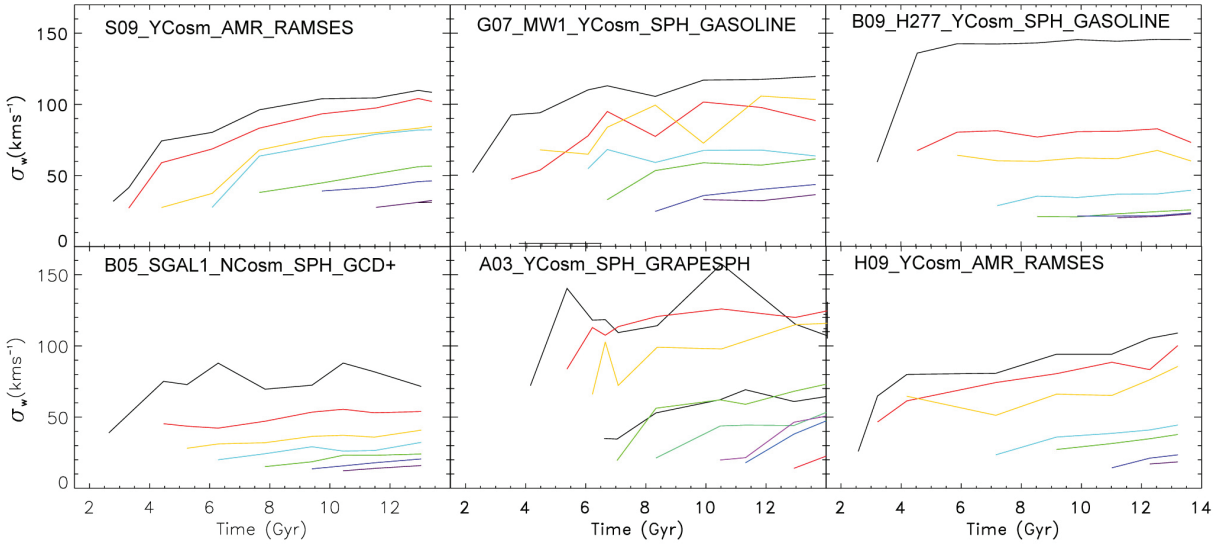

Figure 4. Velocity dispersion perpendicular to the plane (σ_w) of young stars (ages < 200 Myr) at various epochs (represented by different colours and different starting times), traced forward in time to quantify their temporal heating profile.

this simulation undergoes at early times (see Abadi et al. 2003a). The feedback mechanism is not particularly effective and therefore the satellites that merge with the main galaxy contain a large stellar component which affects the high velocity dispersions derived. The merger activity is largely over by ∼6 Gyr and the disc is allowed to settle and form. One can interpret the low velocity dispersions determined in Fig. 3 for stars from $t = 6$ Gyr as a signature of the formation of such disc.

Having identified the velocity dispersions of stars *at birth*, we now wish to determine whether they maintain the self-same dispersion as they age, that is, are these stars being heated with time? We do this by selecting the same 'young' stars at a particular time and then tracing them forward in time, in order to quantify the degree of evolution in the velocity dispersion of these ensembles of stars. This is shown in Fig. 4, where the subsequent heating of the stars at each epoch is represented by the coloured curves. Because we are interested in stars born in the disc of the galaxy, we necessarily choose epochs after the disc has formed, with the exception of A03 where the disc forms much later compared to the other simulations. For each galaxy, this time can vary depending upon the time of the LMM. We therefore do not look at stars beyond $z \sim 2.5$, because, in general, the discs in these galaxies have not yet formed.

Looking first at the S09 simulation, the stars born at $t = 2.5$ Gyr have an initial velocity dispersion of $\sigma_w = 30$ km s^{-1}, increasing to $\sigma_w = 70$ km s^{-1} over the subsequent ∼2 Gyr. This behaviour is qualitatively repeated for all stars born (and tracked) in the first ∼6 Gyr, that is, stars are born relatively cold but rapidly heat to more than double their initial velocity dispersion within ∼1 Gyr, before the heating begins to 'saturate', while stars born over the past ∼6 Gyr (while also born 'cold') heat much more gradually. Indeed, stars born over the last ∼4 Gyr experience essentially no kinematic heating.

G07(MW1) presents a qualitatively similar heating profile to that of S09, in the sense of (a) older stars experiencing a doubling of their vertical velocity dispersion in the first few Gyr after birth, before the heating saturates; and (b) younger stars experiencing little, if any, kinematical heating. One subtle difference between G07(MW1) and S09, though, is that older stars in the former are born relatively hot compared with their younger counterparts, while in S09, all stars, independent of the birth epoch, are born with essentially the same vertical velocity dispersion.

A03 is similar to G07(MW1) in the sense that older stars are born relatively hot compared to the younger stars in the disc. The difference in this simulation compared to both S09 and G07(MW1) is that the younger stars also experience heating, where their dispersions double in the first few Gyr. It can be seen that even stars born at $t = 13$ Gyr are being heated with time (see the red curve in the bottom middle panel of Fig. 4).

Both B09(h277) and B05(SGAL1) present somewhat different heating profiles. With the exception of the first epoch in both (coinciding with the time of the LMM in both cases), the vertical velocity dispersion is essentially invariant, that is, older stars [which are born hotter than their contemporary counterparts, as in G07(MW1)] and younger stars maintain their birth velocity dispersion for the lifetime of the simulation.

The next question which needs addressing is this: what are the responsible agents driving the assorted heating profiles seen in Fig. 4? What is the quantitative relationship to their respective merger histories? Is the effect of warps playing an important role? Are numerical effects plaguing the analysis? We address these over the following subsections.

3.3 The effects of mergers

As noted above, our efforts have concentrated upon the out-of-plane heating within the simulations, due to its stronger sensitivity to mergers and interactions. It is crucial to derive and quantify the merger histories of our simulations, in order to link the observed heating trends with the interactions they have experienced during their evolution.

We have already seen indirect signatures of mergers in the above analysis. Stars born with hotter kinematics during early stages of a galaxy's evolution (Fig. 3), as well as the dramatic heating of stars born at early times over fairly short time-scales (Fig. 4), can be related to the LMM of each galaxy (see Table 1 for the look-back time, $t_{\rm LMM}$, at which the LMM occurred for each simulation). Major mergers have a total mass ratio of 3:1 or higher.

In what follows, we examine minor mergers of satellites with mass 4 per cent the mass of the disc at the time of the merger, back to $z \sim 2$. Such mergers are able to disturb disc structure (Quinn et al. 1993). We are, unfortunately, limited by time-resolution due to the available number of outputs for each simulation. We are thus not able to trace directly the trajectories of the satellites and determine whether they penetrate the disc, or the number of close passages which occur prior to the final coalescence. We restrict our analysis to satellites which have contributed stars to the inner 10 kpc of the central galaxy by $z = 0$, indicating that these satellites have interacted with the disc.

The LMM in the S09 simulation occurs at a look-back time of $t_{\rm LMM} = 10.99$ Gyr, which corresponds to a time $t = 2.02$ Gyr in Fig. 3. It has a mass ratio of 3:1 ($M_{\rm vir} = 1.1 \times 10^{11}$ and $M_{\rm sat} = 1.7 \times 10^{10}$). This major merger heats the disc stars significantly as can be seen in the black line in the top left-hand panel in Fig. 3. After the LMM, there are several minor baryonic mergers, the most noteworthy of which occurs between redshifts $z = 0.8$ and 0.7 (a time corresponding to ∼6.3 Gyr in Fig. 3). This minor merger has a mass ratio of 8:1 ($M_{\rm vir} = 5.7 \times 10^{11}$ and $M_{\rm sat} = 6 \times 10^{10}$). Stars born during this period are somewhat hotter, kinematically speaking, relative to those born before and after (Fig. 3). In addition, stars born in the preceding ∼3 Gyr to this merger appear to have been subject to rapid heating (see the yellow and cyan lines in upper left-hand panel of Fig. 4). Additional (less significant in terms of mass) mergers occur at redshift $z = 1.75$–1.44, that is, $t = 4$–4.5 with a mass ratio of 16:1. The effects of these mergers are not obvious in our plots, although the impact of the former likely plays a role in the heating seen between the times 3 and 4 Gyr in the upper left-hand panel of Fig. 4. This simulation undergoes minor mergers up to redshift $z = 0$.

G07(MW1) undergoes its LMM at a look-back time $t_{\rm LMM} = 10.89$ Gyr, which corresponds to time $t = 2.5$ Gyr in Fig. 3. This major merger has a mass ratio of 3:1 ($M_{\rm vir} = 9 \times 10^{10}$ and $M_{\rm sat} = 2.5 \times 10^{10}$), where the heating caused by this merger can be seen as the increase in the dispersion for stars during this period (see the black line in the top middle panel of Fig. 3). It undergoes several minor mergers at time $t = 3.2$ Gyr with the mass ratios of 10:1 and 15:1, the effects of which can also be seen in Figs 3 and 4. Hereafter, it undergoes minor interactions, the last one occurring at $t = 7.68$ Gyr. These interactions are apparent near $t = 8$ Gyr in Figs 3 and 4, although their heating 'impact' is not particularly obvious in Fig. 3, that is, the stars born at $t = 8$ Gyr (upper middle panel of Fig. 3) are not kinematically hotter than those born within ∼2 Gyr of these mergers; similarly, the impact on the heating of these stars is not particularly dramatic (upper middle panel of Fig. 4). The effect that the LMM (at $t \sim 2.5$ Gyr) has in heating the ISM of G07(MW1) is felt over the subsequent ∼3 Gyr (Fig. 3) and impacts upon the temporal heating profiles of stars born during this period as well (Fig. 4). G07(MW1) hosts fairly significant warps during and after these periods of merger-driven activity, the impact of which has been noted previously (Section 3.2).

For B09(h277) there is a clear distinction between stars born at early times and those formed at later times, which can be ascribed to the simulation's merger history. The LMM in this simulation occurs at a formation time of $t_{\rm LMM} = 10.41$ Gyr, corresponding to time $t = 3.2$ Gyr in Fig. 3 and has a mass ratio of 3:1 ($M_{\rm vir} = 6 \times 10^{10}$ and $M_{\rm sat} = 2 \times 10^{10}$). During the period between $t = 2$ and 3.4 Gyr, a significant number of both major and minor interactions take place, with a final baryonic interaction at $t \sim 3.4$ Gyr (with a mass ratio of 100:1). This period of merger activity maps directly on to the time during which the ISM is significantly hotter (upper right-hand panel of Fig. 3). The complete lack of major or minor baryonic mergers subsequent to this point is reflected in the absence of detectable temporal heating in stars born since $t \sim 4$ Gyr.

We have already discussed the similarity between the heating profiles of B05(SGAL1) and B09(h277), where there is a clear distinction between stars born at early epochs and those born later. B05(SGAL1) has its LMM at a formation time of $t_{\rm LMM} = 9.74$ Gyr or $t \sim 3.3$ Gyr in Fig. 3 and has a mass ratio of 3:1 ($M_{\rm vir} = 6 \times 10^{10}$ and $M_{\rm sat} = 2 \times 10^{10}$). It experiences only one minor 10:1 ($M_{\rm vir} = 6 \times 10^{10}$ and $M_{\rm sat} = 2 \times 10^{9}$) baryonic interaction at $t \sim 6$ Gyr after the LMM, the signature of which is not readily seen in Fig. 3 or 4.

A03 undergoes the LMM with the mass ratio 3:1 at $t \sim 6$ Gyr and it lasts for ∼1 Gyr. The ISM is hotter during this LMM phase, as evidenced in the higher σ_w at time $t \sim 6.5$ Gyr in the lower middle panel of Fig. 3. At times earlier than $t \sim 6$ Gyr, there are many major merger events as can be seen by the large velocity dispersions measured for these stars. It undergoes it last merger event at $z \sim 0.74$, that is, $t = 7.5$ Gyr in Figs 3 and 4, and has completely merged with the disc of the main galaxy by $z \sim 0.48$, that is, $t = 9.2$ Gyr, with a mass ratio of 45:1 ($M_{\rm vir} = 9 \times 10^{11}$ and $M_{\rm sat} = 2 \times 10^{10}$). See Abadi et al. (2003b) for details of this satellite. The heating profile of stars formed more recently in A03 (i.e. those formed within the final 3−4 Gyr of the simulation) differs from those of the other simulations, in the sense that even these recently formed stars within A03 experience significant heating. This can be associated to a companion satellite that survives at $z = 0$. It first appears within a radius of 15 kpc at $z = 0.33$, that is, $t = 10.52$ Gyr, with a mass of $M_{\rm sat} = 5.8 \times 10^{9}$.

We separate our simulations into two groups, those which have interactions at low redshift after the thin disc has formed and those that show no major or minor interactions since redshift $z \sim 1$. S09 (and H09), G07(MW1) and A03 undergo later minor merger interactions and therefore exhibit more evidence of continual, later, heating. Conversely, B09(h277), B05(SGAL1) and R08 (not shown) experience no later minor merger activity once the disc has formed and therefore do not show jumps in the heating over short timescales in their respective discs at later times, which is associated with such merger events in the other simulations. If we combine this information with what we deduce from looking at the age–velocity dispersion plane in Figs 1 and 2, we can conclude that in order to obtain a thin disc consistent with observations, the simulated galaxy must experience no interactions at late times (at least, since $z \sim 1$).

3.4 The central concentration of the satellites

The effect of heating that accreted satellites have on the disc is dependent on the mass distribution of the satellite, in the sense that the accretion of more massive, and more concentrated satellites, will cause a higher degree of heating (e.g. Velazquez & White 1999). Simulations produce rotation curves that rise rapidly in the inner regions with a central peak before dropping off (e.g. Mayer, Governato & Kaufmann 2008). However, observations of dwarf galaxies have shown that their rotation curves rise linearly in the central regions. Presumably, accreted satellites should have mass distributions which are similar to local galaxies. The more concentrated satellites in the simulations are related to the 'angular momentum problem', where the baryons are deficient in angular momentum and produce overly concentrated stellar bulges. This challenge for CDM cosmology is beyond the scope of this paper, but we note that several mechanisms have been proposed to resolve the discrepancy between theory and observation (e.g. Navarro, Frenk & White 1996; Mashchenko, Wadsley & Couchman 2008;

Scannapieco et al. 2009). Governato et al. (2010) showed that the resolution which is high enough for local star formation within an inhomogeneous ISM will drive large-scale SN outflows and decrease the central mass concentration, producing simulated dwarfs which have a mass distribution that matches observed galaxies. The resolution required to create such dwarfs is not achieved in any simulation of a Milky Way mass galaxy in our study, or indeed in the literature.

We looked at the rotation curves of satellites in three of the simulations discussed in this paper, chosen at redshift $z \sim 2$, each with a dynamical mass of $\sim 10^{10}\,M_{\odot}$ and they showed peaked rotation curves indicative of an excess of central material. We have shown that the major source of disc heating in our suite of simulations is due to the interaction and accretion of satellite galaxies with the disc. The high central mass concentration of our satellites may be causing these effects to be exaggerated compared to the effect of real satellites, particularly if such satellites do indeed have 'cored' rather than cuspy central density profiles and no bulge (e.g. Oh et al. 2010). This effect is perhaps the most important caveat to our work; future, increased, resolution which results in more realistic dwarfs (akin to those seen in Governato et al. 2010) may reduce the heating rates seen in the current suite of cosmological simulations.

4 THE EFFECTS OF RESOLUTION AND STAR FORMATION RECIPES

It is important to determine whether numerical heating is influencing our results. Two-body heating can have a dramatic effect on the increase in the kinetic energy of a kinematically cold rotating stellar disc (Mayer 2004) and is therefore an important factor to take into consideration in our study. Such numerical effects are dependent upon resolution (Moore, Katz & Lake 1996; Steinmetz & White 1997).

In our sample of simulations, we have a variety of resolutions. S09, G07(MW1), B05(SGAl1) and A03 have relatively low spatial resolution – between 400 and 600 pc – while B09(h277) and H09 have somewhat higher resolution (∼300 pc). The isolated disc from R08 has a much higher resolution (50 pc). If the heating we see were dominated by numerical effects, one might expect a particularly large effect in the lowest resolution simulation: B05(SGAL1). In fact, this is the coolest of all the simulations studied. Further, we have shown that B09(h277), B05(SGAL1) and R08 present similar trends in the heating of their disc stars during their quiescent period of evolution at low redshift, showing little stellar heating, despite having vastly different resolutions. Of the simulations which show significant recent merger activity, H09 is the highest resolution, yet it shows heating at low redshift in agreement with the lower resolution simulations which have similar merging histories [S09, G07(MW1) and A03]. These trends appear to indicate that numerical heating is not the main driver of the inferred heating profiles.

However, the importance of the spectre of numerical heating is that one must proceed cautiously and examine the issue more quantitatively . In cosmological simulations, resolution dependence is more complicated than the case where isolated discs are used as the initial conditions. There is numerical heating due to gravitational softening, but, on the other hand, when we go to higher resolution we resolve more substructure, creating more heating. Another problem is that low- resolution substructures tend to be (artificially) more concentrated (Barnes & Hernquist 1996; van den Bosch, Burkert & Swaters 2001), meaning that the heating effects of their interactions may be exaggerated. We discussed the central concentrations of the satellites in these cosmological simulations in Section 3.4.

In order to explore possible numerical heating effects, we therefore examined a set of isolated disc galaxies. The initial conditions were created as in Kazantzidis et al. (2008), to which the reader is referred for details, and were run using GASOLINE. The isolated galaxies that we re-simulate comprises an exponential stellar disc, a Hernquist model bulge (Hernquist 1990) and a NFW dark matter profile (Navarro, Frenk & White 1997). The total mass of the galaxy is $10^{12}\,M_{\odot}$, similar to that of the Milky Way, with a disc gas fraction of 10 per cent. To form a rotationally supported disc, we impart angular momentum to the gas component corresponding to a spin parameter of $\lambda = 0.04$. We evolve each simulation for 1 Gyr, after allowing 0.2 Gyr for the system to relax. The disc has an initial Toomre stability parameter equal to $Q = 2.2$, which means it is stable against any local non-axisymmetric instabilities. The main differences between the isolated runs are summarized in Table 2. We run three simulations at different resolutions – high (ISO_HR_LT_GASOLINE), medium (ISO_MR_LT_GASOLINE) and low (ISO_LR_LT_GASOLINE) – and we employ the same star formation threshold ($0.1\,\mathrm{cm}^{-3}$) used in the cosmological simulations analysed in this study. The purpose of this is to see the effects resolution might have on heating stars in simulations. We then run another high-resolution simulation, but employ a much higher star formation threshold ($100\,\mathrm{cm}^{-3}$: ISO_HR_HT_GASOLINE), more comparable to the densities associated with star formation, observationally.

In Fig. 5, we plot the age–velocity dispersion relation for stars within our set of isolated Milky Way disc galaxies. While there is a not surprising resolution dependency in the vertical velocity dispersions of the stars at birth (ranging from ∼16 to ∼21 to ∼29 $\mathrm{km\,s}^{-1}$ for the HR, MR and LR runs, respectively), there is little, if any, evidence for any significant heating within any of the simulations, irrespective of their different resolutions. We will return to the differences that resolution has upon the stellar velocity dispersions at birth, at the end of this section.

The differences in the velocity dispersions between the isolated runs seen in Fig. 5 could be due to the effects of feedback in these simulations. In order to determine how important this effect may be when determining the dispersion in Fig. 5, we compare the SFRs

Table 2. Summary of the properties of the isolated simulations.

Simulation name	Star mass ($M_{\odot}$)	Gas mass ($M_{\odot}$)	Dark mass ($M_{\odot}$)	ϵ^a (kpc)	ϵ^b (kpc)	Star formation threshold (cm^{-3})
ISO_HR_HT_GASOLINE	1.73×10^3	2.56×10^4	1.35×10^5	0.1	0.17	100
ISO_HR_LT_GASOLINE	1.73×10^3	2.56×10^4	1.35×10^5	0.1	0.17	0.1
ISO_MR_LT_GASOLINE	1.38×10^4	2.05×10^5	1.08×10^6	0.2	0.34	0.1
ISO_LR_LT_GASOLINE	1.04×10^5	1.63×10^6	8.68×10^6	0.4	0.68	0.1

[a]Dark matter softening length.
[b]Gas softening length.

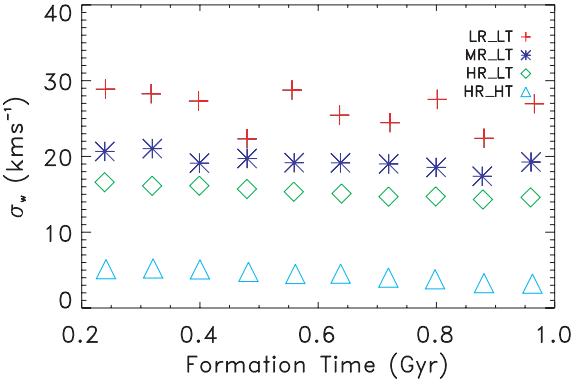

Figure 5. Age–velocity dispersion relation in the vertical direction for disc stars ($4 < R_{xy} < 8$ kpc and $|z| < 1$ kpc) for four isolated Milky Way scale simulations.

in all the isolated runs. We find that the dispersion is not greatly affected by the feedback in the sense that, for example, changes in the SFR (by factors of 2–4) did not change the dispersions. Further, by a comparison between the low and high threshold (HT) dispersions at times when they had equivalent SFRs, we find the same offsets as indicated in Fig. 5.

The highest resolution, isolated simulation, like the case of R08, is particularly interesting in the context of this section. Both these have significantly higher resolution than the cosmological simulations. ISO_HR_LT_GASOLINE and R08 are both isolated from a cosmological context, and so no heating from satellites occurs; yet these simulations have a vertical velocity dispersion 'floor' of $\sim$15–20 km s^{-1}, similar to the 'floor' in dispersions seen in the fully cosmological simulations during their respective quiescent periods. R08 uses the same star formation and SN feedback physics as G07(MW1) and B09(h277); this dispersion 'floor' is tied directly to the implementation of ISM physics within the code. Such physics is difficult to capture in cosmological simulations, as it is multiscale, going from kpc-scale, where most of the gas is ionized, to pc-scale, where most of the gas is molecular. Cosmological simulations, like the ones analysed here, follow the formation of galaxies in a volume of at least several tens of Mpc, because aspects of structure formation require that the large-scale gravitational field is properly modelled. Related to this, our inability to resolve locally collapsing high-density regions means that we average star formation over large columns, using a low density threshold for star formation (0.1 cm^{-3} in the simulations analysed here). Yet star formation is observed to occur in regions where gas has cooled to regions of significantly higher density. The low star formation threshold means that, within the simulations, gas may be forming stars in regions which remain relatively hot.

Recently, Governato et al. (2010) showed that with a spatial resolution of about $\sim$100 pc, gas could be allowed to collapse to densities more representative of the average density observed in star-forming giant molecular clouds. Using a star formation density threshold of 100 cm^{-3}, they successfully simulated the first bulgeless disc galaxy (see Governato et al. 2010 and Brook et al. 2010). However, if the density threshold is too high for the resolution of the simulation, the galaxy comes out too compact. We implement these HT recipes within a high-resolution isolated simulation (ISO_HR_HT_GASOLINE), and overplot the age–velocity dispersion relationship (cyan triangles) in Fig. 5 . Two striking features are immediately apparent: (i) the dispersion is much lower than for all the simulations which used a low star formation density threshold, even when using the same high resolution. The difference is far greater than the difference which was caused by resolution[5]; and (ii) very little heating occurs, even at these very low dispersions. This shows very clearly that numerical heating is not affecting our cosmological simulations. Rather, a dispersion floor is created by the inability of gas to cool sufficiently before forming stars when the star formation density threshold is set at a lower level (0.1 cm^{-3}).

The resolution-dependent differences in the dispersions of the isolated simulations are due to the differences in the degree to which the gas is able to cool before forming stars. This is supported by three pieces of information: (i) no heating is apparent at any of the three significantly different resolutions, with the age-velocity -dispersion relation remaining flat; (ii) stars form with lower dispersion at higher resolution; and (iii) even at the very low dispersion levels of the HT simulation ($\sim$5 km s^{-1}), heating was negligible. These conclusions are supported by the fact that the temperature of the gas from which stars are born increases, as resolution decreases, with the average temperature being 7300, 6500, 5900 and 400 K, respectively, for the LR, MR, HR and HR_HT isolated galaxies.

5 SUMMARY

We have analysed the kinematics of disc stars in a suite of Milky Way scale simulations which were run with different hydrodynamical cosmological codes and at different resolutions. Some were run using the SPH approach, whereas others used the AMR method. This is the first paper to compare cosmological disc galaxies run with these two different techniques. No differences in the analysed kinematic properties of the simulated galaxies were found to be dependent on the approach used for the implementation of gas hydrodynamics.

First, we analysed the velocity dispersion of all disc stars as a function of age at $z = 0$, comparing with analogous observations of the Milky Way's disc. An overall offset exists, in the sense that all the simulated galaxies are hotter than the Milky Way's disc. This was shown to be driven in part by resolution and star formation threshold effects, although the latter is much more efficient at reducing the dispersion 'floor' (Fig. 5). We provide evidence that the dominant contributor is the low density threshold for star formation, which has been routinely implemented in simulations of Milky Way scale galaxies, although we should point out that we only show this for non-cosmological simulations. This low density threshold means that stars are formed from unphysically high temperature gas, creating a dispersion 'floor'. Indeed, our lowest resolution simulation has the least amount of kinematical heating. Future cosmological simulations with sufficient resolution to resolve the mean density of giant molecular clouds [akin to the Governato et al. (2010) dwarf galaxy simulations] will be a critical step forward in this work.

Despite this dispersion 'floor' in our simulations, some interesting heating trends are found. Two of our simulations [B09(h277) and B05(SGAL1)] are in better agreement with interpretations made by Quillen & Garnett (2001), where a saturated disc is present for young stars up to $t = 6$ Gyr and discrete jumps seen in the dispersion for older disc stars. The other simulations [S09, G07(MW1), A03 and R08] seem to be in better agreement with the disc undergoing continuous heating, consistent with the analysis of Holmberg

[5] See Pilkington et al. (in preparation) for a detailed analysis of the ISM velocity dispersion as a function of the star formation threshold and resolution.

et al. (2008), although the rate of heating in the simulations remains higher than that observed in nature.

We then proceeded to study the heating of these stars as a function of time; starting from the point at which the final disc was stable ($z \sim 2$), we derived the dispersion of stars at the time of their birth and how those coeval ensembles evolved with time. We found that whereas in some simulations stars are born cold in the disc and are heated [S09, G07(MW1), A03 and H09], either numerically or due to a physical process, in other simulations [B09(h277), B05(SGAL1) and R08], the stars maintain essentially the same dispersion as they possessed at birth. Further, in some simulations, stars are born with high dispersions, that is, they are born 'hot'. This can be due to interactions (Brook et al. 2004b) and/or warps (Roškar et al. 2010). Turbulence in the ISM not related to mergers could also be a cause of stars being born with large velocity dispersion. Recent observations of high-redshift discs indicate that internal processes are a possible cause of the observed turbulent ISM (Genzel et al. 2008). Bournaud, Elmegreen & Martig (2009) compared simulations formed internally in unstable gas-rich, clumpy discs with simulations of merger-induced disc thickening, and found that thick discs formed internally are a better match to observed high-redshift discs. Mechanisms such as cold flows and SN feedback are currently being discussed – in addition to mergers – as possible causes of the turbulent ISM in high-redshift systems (Burkert et al. 2010; Ceverino, Dekel & Bournaud 2010; Förster Schreiber et al. 2011).

Within the favoured cosmological paradigm of hierarchical clustering, the merging and accretion of satellites on to host galaxies is fundamental. Our goal has been to examine the effects that these mergers might have upon the heating of disc stars. We find a clear relationship when looking at the heating profiles between those simulations that have late mergers and those that heat significantly. Four simulations [S09, G07(MW1), A03 and H09] have minor mergers at low redshift and we map these interactions on to the increases seen in the velocity dispersion of their disc stars. The other three simulations [B09(h277), B05(SGAL1) and R08], which have no interactions over the past $\sim$7 Gyr, show little heating in the disc with time. We note that R08 is an isolated simulation which has no satellites, and hence no interactions, yet has sufficient heating due to spiral arms and migration to match observed heating rates of the Milky Way. The suite of cosmological simulations do not have the ability to resolve these secular effects, nor heating due to molecular clouds. In these simulations, it is only in the quiescent period since the last accretion events that heating is low enough to match the Milky Way's thin disc (see also Kormendy et al. 2010). None has a thin disc older than $\sim$6 Gyr, indicating that it would be difficult to gain a thin disc as old as some estimates for the Milky Way thin disc within the current CDM paradigm. A caveat of our study is the overly concentrated mass distributions of our satellites, meaning that the resolution of this persistent 'old thin disc' problem may come from improved modelling of baryonic physics coupled with increased resolution.

ACKNOWLEDGMENTS

We thank F. Calura for helpful conversations and suggestions during this project. ELH acknowledges the support of the UK's Science & Technology Facilities Council through its PhD studentship programme (ST/F006764/1). BKG and CBB acknowledge the support of the UK's Science & Technology Facilities Council (ST/F002432/1). The simulations analysed here were made possible by the University of Central Lancashire's High Performance Computing Facility, the UK's National Cosmology Supercomputer (COSMOS), NASA's Advanced Supercomputing Division, TeraGrid, the Arctic Region Supercomputing Center and the University of Washington. PS-B acknowledges the support of a Marie Curie European Reintegration grant within the Sixth European Community Framework Programme. FG acknowledges the support from the HST GO-1125, NSF AST-0607819 and NASA ATP NNX08AG84G grants. RT would like to thank the granted access to the HPC resources of CINES and CCRT under the allocations 2009-SAP2191 and 2010-GEN2192 made by GENCI. We thank the DEISA consortium, co-funded through EU FP6 project RI-031513 and the FP7 project RI-222919, for support within the DEISA Extreme Computing Initiative.

REFERENCES

Abadi M. G., Navarro J. F., Steinmetz M., Eke V. R., 2003a, ApJ, 591, 499
Abadi M. G., Navarro J. F., Steinmetz M., Eke V. R., 2003b, ApJ, 597, 21
Agertz O., Teyssier R., Moore B., 2010, preprint (ArXiv e-prints)
Anguiano B., Freeman K., Steinmetz M., Wylle de Boer E., Siebert A., The Rave Collaboration, 2009, in Andersen J., Bland-Hawthorn J., Nordström B., eds, Proc. IAU Symp. 254, The Galaxy Disk in Cosmological Context. Cambridge Univ. Press, Cambridge, p. 3
Aumer M., Binney J. J., 2009, MNRAS, 397, 1286
Bailin J. et al., 2005, ApJ, 627, L17
Barnes J. E., Hernquist L., 1996, ApJ, 471, 115
Beers T. C., Lee Y. S., Peruta C., Sivarani T., Allende Prieto C., Aoki W., Carollo D., SDSS 2009, BAAS, 41, 228
Bensby T., Feltzing S., Lundström I., 2003, A&A, 410, 527
Bensby T., Feltzing S., Lundström I., 2004, A&A, 415, 155
Bensby T., Zenn A. R., Oey M. S., Feltzing S., 2007, ApJ, 663, L13
Bournaud F., Elmegreen B. G., Martig M., 2009, ApJ, 707, L1
Brook C. B., Kawata D., Gibson B. K., Flynn C., 2004a, MNRAS, 349, 52
Brook C. B., Kawata D., Gibson B. K., Freeman K. C., 2004b, ApJ, 612, 894
Brook C. B., Gibson B. K., Martel H., Kawata D., 2005, ApJ, 630, 298
Brook C., Governato F., Roškar R., Brooks A., Mayer L., Quinn T., Wadsley J., 2010, in Debattista V. P., Popescu C. C., eds, AIP Conf. Ser. Vol. 1240, Hunting for the Dark: The Hidden Side of Galaxy Formation. Am. Inst. Phys., New York, p. 203
Brooks A. M., Governato F., Quinn T., Brook C. B., Wadsley J., 2009, ApJ, 694, 396
Burkert A. et al., 2010, ApJ, 725, 2324
Carollo D. et al., 2010, ApJ, 712, 692
Ceverino D., Dekel A., Bournaud F., 2010, MNRAS, 404, 2151
Chiba M., Beers T. C., 2000, AJ, 119, 2843
Dalcanton J. J., Bernstein R. A., 2002, AJ, 124, 1328
Dehnen W., Binney J. J., 1998, MNRAS, 298, 387
Edvardsson B., Andersen J., Gustafsson B., Lambert D. L., Nissen P. E., Tomkin J., 1993, A&AS, 102, 603
Elmegreen B. G., 2007, ApJ, 668, 1064
Elmegreen B. G., Elmegreen D. M., 2006, ApJ, 650, 644
Förster Schreiber N. M., Shapley A. E., Erb D. K., Genzel R., Steidel C. C., Bouché N., Cresci G., Davies R., 2011, ApJ, 731, 65F
Genzel R. et al., 2008, ApJ, 687, 59
Gibson B. K., Courty S., Sánchez-Blázquez P., Teyssier R., House E. L., Brook C. B., Kawata D., 2009, in Andersen J., Bland-Hawthorn J., Nordström B., eds, Proc. IAU Symp. 254, Hydrodynamical Adaptive Mesh Refinement Simulations of Disk Galaxies. P. 445
Gilmore G., Reid N., 1983, MNRAS, 202, 1025
Governato F., Willman B., Mayer L., Brooks A., Stinson G., Valenzuela O., Wadsley J., Quinn T., 2007, MNRAS, 374, 1479
Governato F. et al., 2010, Nat, 463, 203
Hernquist L., 1990, ApJ, 356, 359
Holmberg J., Nordström B., Andersen J., 2007, A&A, 475, 519
Holmberg J., Nordstroem B., Andersen J., 2008, VizieR Online Data Catalog, 5128, 0

Ivezić Ž. et al., 2008, ApJ, 684, 287
Jurić M. et al., 2008, ApJ, 673, 864
Katz N., Hernquist L., Weinberg D. H., 1992, ApJ, 399, L109
Kawata D., Gibson B. K., 2003, MNRAS, 340, 908
Kazantzidis S., Bullock J. S., Zentner A. R., Kravtsov A. V., Moustakas L. A., 2008, ApJ, 688, 254
Kazantzidis S., Zentner A. R., Kravtsov A. V., Bullock J. S., Debattista V. P., 2009, ApJ, 700, 1896
Knebe A., 2005, Proc. Astron. Soc. Aust., 22, 184
Kormendy J., Drory N., Bender R., Cornell M. E., 2010, ApJ, 723, 54K
Kroupa P., 2002, Sci, 295, 82
Larson R. B., 1976, MNRAS, 176, 31
Lemoine-Busserolle M., Lamareille F., 2010, MNRAS, 402, 2291
Loebman S. R., Roskar R., Debattista V. P., Ivezic Z., Quinn T. R., Wadsley J., 2010, preprint (arXiv:1009.5997)
Mashchenko S., Wadsley J., Couchman H. M. P., 2008, Sci, 319, 174
Mayer L., 2004, preprint (astro-ph/11476M)
Mayer L., Governato F., Kaufmann T., 2008, 801, preprint (arXiv:0801.3845)
Moore B., Katz N., Lake G., 1996, ApJ, 457, 455
Moster B. P., Macciò A. V., Somerville R. S., Johansson P. H., Naab T., 2010, MNRAS, 403, 1009
Navarro J. F., Benz W., 1991, ApJ, 380, 320
Navarro J. F., White S. D. M., 1994, MNRAS, 267, 401
Navarro J. F., Frenk C. S., White S. D. M., 1996, ApJ, 462, 563
Navarro J. F., Frenk C. S., White S. D. M., 1997, ApJ, 490, 493
Navarro J. F., Abadi M. G., Venn K. A., Freeman K. C., Anguiano B., 2011, MNRAS, 412, 1203
Nissen P. E., 1995, in van der Kruit P. C., Gilmore G., eds, Proc. IAU Symp. 164, Age and Metallicity Distributions among Galactic Disk Stars. Kluwer, Dordrecht, p. 109
Nordström B. et al., 2004, A&A, 418, 989
Oh S.-H., Brook C., Governato F., Brinks E., Mayer L., de Blok W. J. G., Brooks A., Walter F., AJ, preprint (arXiv:1011.2777)
Okamoto T., Eke V. R., Frenk C. S., Jenkins A., 2005, MNRAS, 363, 1299
Purcell C. W., Bullock J. S., Kazantzidis S., 2010, MNRAS, 404, 1711
Quillen A. C., Garnett D. R., 2001, in Funes J. G., Corsini E. M., eds, ASP Conf. Ser. Vol. 230, The Saturation of Disk Heating in the Solar Neighborhood and Evidence for a Merger 9 Gyr Ago. Astron. Soc. Pac., San Francisco, p. 87
Quinn P. J., Hernquist L., Fullagar D. P., 1993, ApJ, 403, 74
Read J. I., Lake G., Agertz O., Debattista V. P., 2008, MNRAS, 389, 1041
Reddy B. E., Tomkin J., Lambert D. L., Allende Prieto C., 2003, MNRAS, 340, 304
Reid N., Majewski S. R., 1993, ApJ, 409, 635
Robertson B. E., Kravtsov A. V., 2008, ApJ, 680, 1083
Robertson B., Yoshida N., Springel V., Hernquist L., 2004, ApJ, 606, 32
Roškar R., Debattista V. P., Quinn T. R., Stinson G. S., Wadsley J., 2008, ApJ, 684, L79
Roškar R. et al., 2008, ApJ, 675, L65
Roškar R., Debattista V. P., Brooks A. M., Quinn T. R., Brook C. B., Governato F., Dalcanton J. J., Wadsley J., 2010, MNRAS, 408, 783
Sánchez-Blázquez P., Courty S., Gibson B. K., Brook C. B., 2009, MNRAS, 398, 591
Scannapieco C., Tissera P. B., White S. D. M., Springel V., 2009, in Andersen J., Bland-Hawthorn J., Nordström B., eds, Proc. IAU Symp. 254, The Galaxy Disk in Cosmological Context. Cambridge Univ. Press, Cambridge, p. 369
Schönrich R., Binney J., 2009, MNRAS, 396, 203
Seabroke G. M., Gilmore G., 2007, MNRAS, 380, 1348
Sommer-Larsen J., Götz M., Portinari L., 2003, ApJ, 596, 47
Soubiran C., Girard P., 2005, A&A, 438, 139
Soubiran C., Bienaymé O., Mishenina T. V., Kovtyukh V. V., 2008, A&A, 480, 91
Springel V., Di Matteo T., Hernquist L., 2005, MNRAS, 361, 776
Steinmetz M., 1996, MNRAS, 278, 1005
Steinmetz M., Mueller E., 1994, A&A, 281, L97
Steinmetz M., Navarro J. F., 2002, New Astron., 7, 155
Steinmetz M., White S. D. M., 1997, MNRAS, 288, 545
Stewart K. R., Bullock J. S., Wechsler R. H., Maller A. H., 2009, ApJ, 702, 307
Summers F. J., Evrard A. E., Davis M., 1993, in Shull J. M., Thronson H. A., eds, The Evolution of Galaxies and their Environment Galaxy Tracers in N-body simulations. 56
Teyssier R., 2002, A&A, 385, 337
van den Bosch F. C., Burkert A., Swaters R. A., 2001, MNRAS, 326, 1205
van Starkenburg L., van der Werf P. P., Franx M., Labbé I., Rudnick G., Wuyts S., 2008, A&A, 488, 99
Velazquez H., White S. D. M., 1999, MNRAS, 304, 254
Wadsley J. W., Stadel J., Quinn T., 2004, New Astron., 9, 137
Yoachim P., Dalcanton J. J., 2008, ApJ, 682, 1004
Zolotov A., Willman B., Brooks A. M., Governato F., Hogg D. W., Shen S., Wadsley J., 2010, ApJ, 721, 738

This paper has been typeset from a TEX/LATEX file prepared by the author.